

## Project information

<b>Project full title</b>	Detectors: Joint Development of Detector Technologies
<b>Project acronym</b>	EURIZON
<b>Grant agreement no.</b>	871072
<b>Instrument</b>	Research and Innovation Action (RIA)
<b>Duration</b>	01/02/2020 – 31/1/2024
<b>Website</b>	

## Deliverable information

<b>Deliverable no.</b>	7.6
<b>Deliverable title</b>	Design of demonstrator MAPS tracker for fixed target geometry
<b>Deliverable responsible</b>	GUF
<b>Related Work-Package/Task</b>	WP7, Task 7.1: Development of CMOS technologies for high-rate Silicon trackers [CNRS-IPHC, FAIR, GUF, INR NASU]
<b>Type (e.g. Report; other)</b>	Report, deliverable
<b>Author(s)</b>	Christian Müntz
<b>Author(s) affiliation</b>	GUF
<b>Dissemination level</b>	Public
<b>Document Version</b>	1
<b>Date</b>	24/01/24
<b>Download page</b>	

## Document information

Version no.	Date	Author(s)	Comment
1	24/01/24	Christian Müntz	

## Table of Contents

1 The MIMOSIS tracker .....	2
1.1 Key points of the CBM MVD sensor integration .....	2
1.2 Follow-up studies required .....	2
2 Optimization of TPG surface properties .....	3
3 Machining TPG .....	4
4 The demonstrator tracker .....	5
5 Summary .....	7



## 1 The demonstrator MAPS tracker for fixed target geometry

Micro-Vertex tracking in immediate neighborhood to the primary vertex in a fixed-target geometry translates in facing several challenges w.r.t. radiation hardness of sensors and materials, efficient cooling of sensors and front-end electronics in vacuum, minimal multiple scattering of tracks, and last but not least providing the granularity and redundancy required by the underlying physics questions. The CBM Micro Vertex Tracker MVD addresses these issues. A concept has been developed and documented in the corresponding Technical Design Report in 2021<sup>1</sup>.

### 1.1 Key points of the CBM MVD sensor integration

The CBM MVD comprises four planar detector stations in the target vacuum, equipped with dedicated radiation-hard MAPS called MIMOSIS. They are mounted on both sides of thin carriers, to guarantee full detection coverage inside the geometrical acceptance. The sensors, thinned to 50  $\mu\text{m}$ , are wire-bonded to thin flex cables, routed to the front-end electronics, which is mounted on actively cooled heat sinks, to which the sensor carriers are clamped. This integration concept depends on efficient conductive heat evacuation in the acceptance and hence relies on dedicated carriers, which are both, thin enough to allow for a material budget of 0.3 to 0.5%  $x/X_0$  and thick enough to have the heat produced by the sensors efficiently transported towards the heat sinks, while providing the self-supporting mechanical stability and precision required for a micro-vertex tracker. Two carrier materials are recommended, pCVD diamond and Thermal Pyrolytic Graphite TPG, featuring with about 1500 W/(Km) a heat conductivity high enough to allow for carrier thickness of several 100  $\mu\text{m}$  only which are thin enough to meet the requirements w.r.t. the material budget.

The concept developed for the CBM MVD has been demonstrated with a large full-size prototype station, employing – also for cost reasons – 380  $\mu\text{m}$  TPG. MAPS have been mounted, and operated in vacuum, on both sides. The double-sided assembly of several sensor rows remains challenging and introduces the main risk w.r.t. the sensor integration yield. This concept represents the baseline of the CBM MVD.

### 1.2 Follow-up studies required

During R&D, issues with sensor integration, following the CBM MVD concept, have been identified and suggest further dedicated studies with the focus on TPG. pCVD diamond would allow to reach a bit smaller material budget in this application, but apart from the costs it became obvious that handling 150  $\mu\text{m}$  thick and large-area (e.g., 10x10  $\text{cm}^2$ ) carriers of this material introduces a significant extra risk to the integration process. Hence, pCVD diamond will only be employed for the first small-size sensor station in a fixed-target geometry. TPG, on the other hand, features certain drawbacks, which have been addressed during the project reported here. First, its surface roughness and macroscopic texture calls for systematic studies on coating (Parylene coating to guarantee electrically non-conductive surface, as well as binding graphite dust), adhesion (activation prior to coating or gluing) and gluing for vacuum applications. Second, TPG is, in contrast to pCVD diamond, a rather soft material with consequences of the quality after in machining and cutting. This issue is for high-precision vertex trackers crucial, since, e.g., sensor and carrier positioning has to provide the precision required during assembly as well as during operation. In addition, dedicated options of high-precision machining of TPG would allow to further reduce the material budget of the carrier.

---

<sup>1</sup> [https://edms.cern.ch/file/2738980/LATEST/MVD\\_TDR\\*.pdf](https://edms.cern.ch/file/2738980/LATEST/MVD_TDR*.pdf)



As a consequence, this project has been structured in three work packages, which are being discussed in the following:

- Optimizing the **surface properties** of thin TPG sheets.
- Identifying **machining tools** for TPG to improve high-precision sensor and carrier integration.
- Validating the above mentioned techniques with a dedicated **demonstrator**.

## 2 Optimization of TPG surface properties

TPG features, by production, a textured surface with a residual roughness. Figure 1 (left side) depicts close ups of TPG sheets we purchase from the company MOMENTIVE, typically with a thickness of 380 or 500  $\mu\text{m}$ . Tests with sheets of thicknesses below 380  $\mu\text{m}$  tend to buckle easily and cannot be recommended for our application.

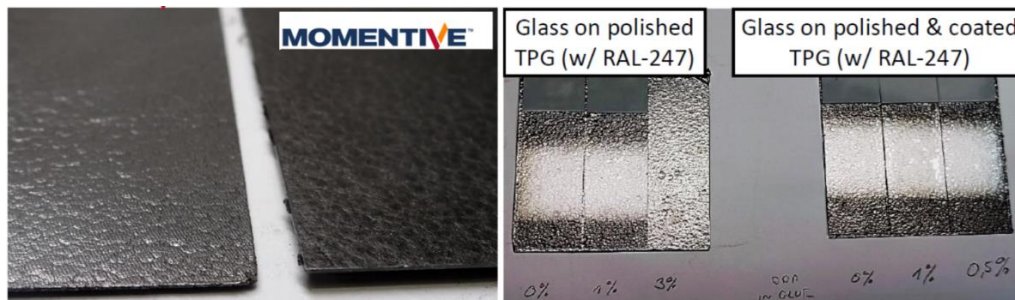


Figure 1: Left: Close ups of TPG sheets, delivered by MOMENTIVE. Right: Tests with surface treatment prior to glue dispensing, with glass sheets to allow for visual inspection and different amounts of wetting agent.

The surface texture as well as the tendency to unravel at edges is clearly visible. The surface roughness does in general not harm gluing of sensors, the glue (RAL-247 in this example, Epo-Tec 301-2 under test as well) with low viscosity before curing will compensate all micro and macro pockets. We have studied (the combination of) two surface treatments, (i) polishing TPG and (ii) Parylene coating ( $< 10 \mu\text{m}$ ). The latter is recommended to provide an electrically non-conductive surface to glue the sensors on, and to avoid spreading of residual conductive dust (TPG graphite subject to abrasion).

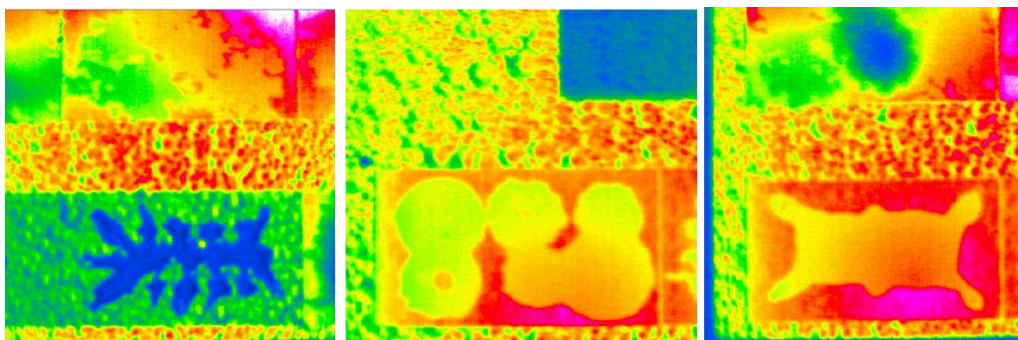


Figure 2: Examples of IR pictures of sensor (Si) dummies glued on TPG with different glue dispensing patterns and TPG surface treatment, confirming IR visualization of examining hidden glue patterns.

However, Parylene is hydrophobic. The optimization tests show satisfying results w.r.t. the glue distribution after curing, which can be studied by visual inspection employing thin glass sheets instead of sensors. Alternatively, IR visualization was employed to systematically study and optimize glue composition and amount, dispensing pattern and curing protocol with sensor (Si) dummies on TPG, see figure 2 showing three examples.

As a result, the preparation of TPG sheets, QA procedures and integration steps of sensors on TPG sheets has been significantly improved. Having assessed the resulting sensor stations with the demonstrator tracker described below, these results are beneficial also for the pre-production phase of the CBM MVD.

### 3 Machining TPG

Besides surface treatment, the limits of machining of TPG prior to sensor placement and gluing has been explored. Reaching precision (typically some 10  $\mu\text{m}$  in this application) and reproducibility is mandatory to (i) assemble the sensors reliably, providing sufficient sensor-to-sensor and sensor-to-carrier alignment, (ii) guarantee a perfect fixation, including thermal bridges, to the heat sink, and (iii) further reduce the material budget by introducing dedicated cut-outs while keeping the vacuum compatibility and efficient heat evacuation.

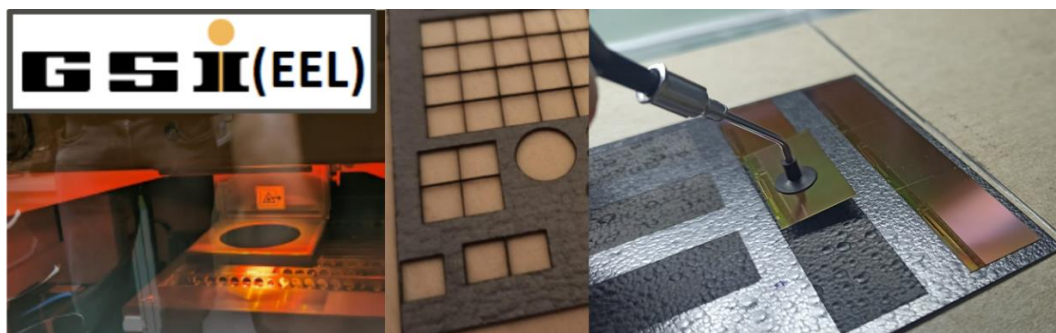


**Figure 3:** Left: Laser ablation device in use at GSI (EEL). Middle: TPG sample with cut-outs to study precision and properties of TPG structures after cutting. Right: TPG sheet surface ablation studies, producing hatches for sensor positioning.

A laser ablation/depaneling (and cutting) device, see figure 3, has been employed to machine TPG sheets of several 100  $\mu\text{m}$  thickness. Structures of about 100  $\mu\text{m}$  width can be cut out, with a precision of about 10  $\mu\text{m}$ , see picture in the middle. On the right side hatches in TPG sheets have been machined, with a depth of 50  $\mu\text{m}$ . Besides reducing the material budget, these hatches ease the relative positioning of sensors w.r.t. each other as well as the distribution of glue. It is important that sensors do not touch each other. In addition, this technique allows to use the TPG carrier itself, by introducing fiducial markers, for sensor and detector alignment purposes. As a side product, this ablation method also allows to remove silicon, i.e., reworking of already glued sensors is possible and would increase the integration yield.

It has been shown, as part of a MSc thesis<sup>2</sup>, that the alignment precision can be significantly improved by means of this new technique applied to thin TPG sheets within this project.

## 4 The demonstrator tracker

In the concluding step of this project the above mentioned new integration techniques have been applied to build a mechanical demonstrator for a MAPS tracker, operational in vacuum with lowest possible material budget. Since the MIMOSIS2 sensors have not been available in this phase of the project, the sensors have been replaced by thinned Si dummies to exercise handling and gluing. Figure 4 depicts the schematic cross section of this device, realized as a  $\mu$ -tracker with two sensors back-to-back, mounted on a dedicated TPG carrier which is clamped into an actively cooled aluminum heat sink (optimized for CBM MVD stations).

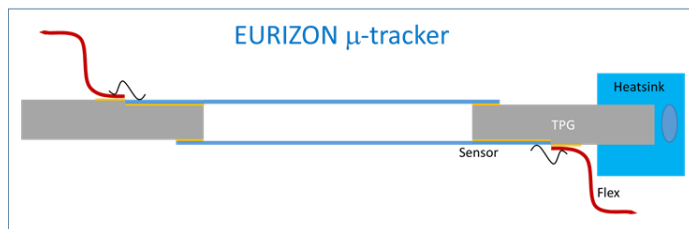


**Figure 4: Schematic cross section of the  $\mu$ -tracker, along A-B in figure 5. Two back-to-back sensors in the middle, mounted on a TPG carrier with cut-out and hatches. Openings along the sides, not visible here, do guarantee vacuum compatibility**

This layout allows to realize and study:

- Pre-treatment of TPG surfaces, e.g., to ease gluing,
- Precision of cutouts in TPG to minimize material budget while keeping vacuum compatibility,
- Employing hatches on one side to support and cool the sensors along its digital part where most of the heat is produced.

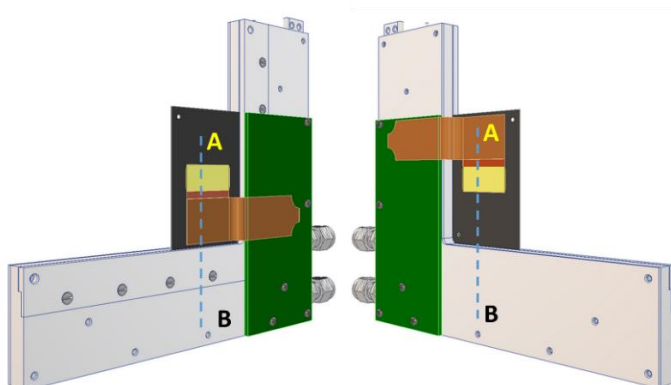


**Figure 5: CAD views of the  $\mu$ -tracker. Yellow: sensors, brownish: flex cables, dark gray: TPG carrier, light gray: heat sink, green: frontend electronics.**

<sup>2</sup> F. Matejcek, MSc thesis to be submitted in February 2024, Goethe-University Frankfurt/Main



Figure 5 shows CAD technical drawings (views) of the  $\mu$ -tracker, indicating the position of the front-end electronics mounted on the heat sink. One important aspect is the evacuation of heat produced by the sensors themselves. Due to intrinsic properties of the sensor, i.e., the arrangement of pixel matrices and the number of individually adjustable detection thresholds, the temperature gradient over the sensor width should not exceed 5 K. Figure 6 studies in a simulation (Inventor Autodesk) the resulting gradients for thinned sensors (50  $\mu\text{m}$ ) and a 380  $\mu\text{m}$  thin TPG carrier. It should be noted that the precision of these simulation in this pseudo-planar application was shown by comparison to measurements to be less than 1 K. The resulting temperature gradient meets the requirements within the simulation's precision.

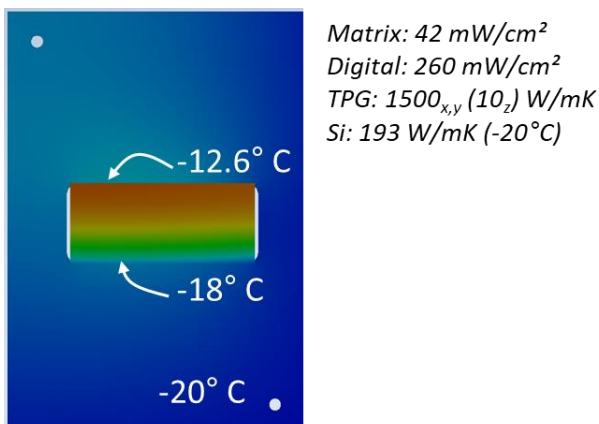


Figure 6: Inventor Autodesk simulation of the thermal behavior of the  $\mu$ -tracker. With the known power consumption of MIMOSIS, and its areal distribution over the sensor, and the heat conductivities of TPG and silicon, a gradient of about 5 K results, well in agreement with the requirements. Si: 50  $\mu\text{m}$ , TPG: 380  $\mu\text{m}$  thick.

Figure 7 shows the mechanical version of the  $\mu$ -tracker described above. All newly developed sensor integration techniques have been employed. Note, the precision of the very small support for the two sensor edges (left/right), to which the sensor is glued.

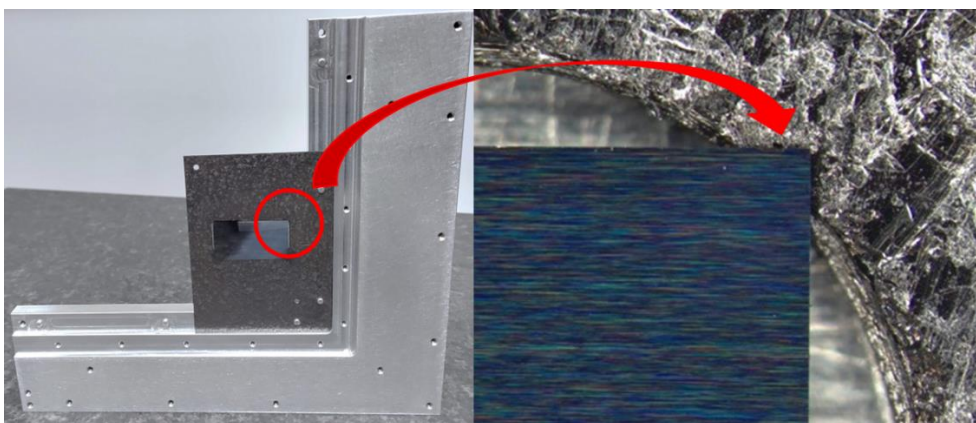


Figure 7: Mechanical realization of the  $\mu$ -tracker (left), right: zoom of one corner indication the small support of the sensors (silicon dummy), two Si dummies have been integrated on both sides of the TPG carrier.

## 5 Summary

Within this work package a demonstrator for a MAPS tracker has been realized. Due to the non-availability of the MIMOSIS2 sensor, the demonstrator has been finally assembled with thinned silicon dummies. However, the focus of this study was the development and assessment of new techniques to integrate thinned sensors in planar detector stations, respecting mounting precision, mechanical precision, vacuum operation, material budget and thermal management, based on the properties of the MIMOSIS MAPS pixel sensor. We have significantly improved on precision and reliability when employing Thermal Pyrolytic Graphite sheets as carrier material for large area planar trackers. With having the demonstrator realized the next step will be to integrate MIMOSIS2 sensors and to operate this device together with a dedicated telescope, or at mini-CBM.

